Design and Experimentation of a Hydrokinetic Turbine for Electricity Generation in Closed Pipes

JAVIER ARMAÑANZAS*, MARINA ALCALÁ, JUAN PABLO FUERTES, JAVIER LEON, ALEXIA TORRES, MIGUEL GIL
Department of Engineering,
Public University of Navarre (UPNA),
Campus de Arrosadia S/N, 31006 Pamplona,
SPAIN

**Corresponding Author*

Abstract: In the present research work, a device for electrical energy generation to be used in water pipelines has been designed, simulated, and tested. To achieve this, a study of the most influential parameters involved in the experiment has been carried out and both, the turbine model and the geometry of the experimental test pipe, have been selected through CFD simulations. Next, the Design of Experiments (DOE) has been used to obtain the configuration with a higher energy extraction from running water. Finally, the turbine and the test pipe section have been manufactured by 3D printing and the experimental tests have been carried out with the optimal configuration to validate the results obtained in the CFD simulations. To simulate the exchange of energy between the water and the turbine, the CFD software SIMULIA XFlow has been used.

Key-Words: - Hydrokinetic turbine, pipe, CFD, Xflow, Lattice-Boltzmann, Design of Experiments (DOE).

Received: February 11, 2023. Revised: November 24, 2023. Accepted: December 22, 2023. Published: February 23, 2024.

1 Introduction

Hydrokinetic turbines integrated in pipelines offer a novel method of harnessing water's energy during internal flow. Such technology garners increasing research attention for its high innovative potential. Nowadays, there has been an increase in new ideas to produce energy at a low scale, which sparked a renewed interest in microgeneration, [1]. Power generation from water flows has evolved constantly, with a spike in recent years. In the present day, hydroelectric turbines are employed in large-scale power generation, whereas hydrokinetic turbines are considered to be a technology more focused on microgeneration, using flows such as rivers, canals, and sea currents. In [1] and [2], a wide state-of-the-art revision regarding the technology used in small hydroelectric plants is displayed, emphasizing in its use among sustainable power systems.

In recent years, there has been a growth in publications about obtaining electricity from microgeneration, and specifically from hydrokinetic turbines, due to the growing investment being made in this technology because of its sustainable nature. In the studies [3] and [4], a thorough review of hydrokinetic energy conversion technologies is carried out, paying special attention to the current research trends and their future perspectives. In [4] is stated that recent progress in hydrokinetic energy conversion has advanced beyond the experimental stage, as it has managed to generate up to 120 TWh per year in the United States.

Based on these premises, a significant amount of research has been concentrated on the design and development of hydrokinetic turbines and their installation areas. Both experimental and numerical simulation techniques have been utilized in these studies, [5], [6], [7], [8], [9], [10], [11], [12]. [5], is solely focused on investigating the design and experimentation of hydrokinetic turbines. They emphasize the practical relevance of this technology and propose optimization strategies for its installation inside channels. In [6], a new full-scale portable hydrokinetic turbine prototype for river applications is examined, conducting both experimental and numerical analyses. [7], provide a review of technologies to harness energy obtained using hydrokinetic turbines. Additionally, in [8], scale models to characterize diverse hydrokinetic turbine designs based on tests completed in a laboratory water channel is utilized. In [9], an approach to evaluate the energy potential and economic viability of hydrokinetic turbines in rivers using numerical predictions and experimental data is presented. In [10], a CFD analysis of a turbine to

determine optimal design parameters is conducted. Lastly, in [11], the design of hydrokinetic turbines installed in ducts using CFD is optimized.

Also, hydrokinetic turbines' practical application across different environments and countries is illustrated in [12], [13], [14], [15], including research cases such as [12] in Malaysia and [13] in the Amazon region. Furthermore, in [14], the momentum recovery in the wake of axial-flow hydrokinetic turbines is analyzed, providing valuable insight into their overall efficiency.

The use of hydrokinetic energy in pipelines looks promising as a form of energy generation with a smaller environmental footprint than other renewable sources, including wind, solar, or conventional hydropower. Several studies have been carried out on the modeling of design and implementation within pipelines, such as [15], [16], and [17], where drag-based, propeller-type, and spherical turbines designs are analyzed, respectively.

As a result, new companies are emerging to produce this type of turbine, [18], [19], [20]. In [21], the model developed by Purdue ECT [20] has been implemented in cities throughout Panama, demonstrating its exceptional performance. Finally, several patents have been registered for electricity-generating devices inside pipelines, [22], [23], [24], [25], [26], [27], indicating ongoing research to improve and diversify these designs.

This study centers on the electric power generated by a hydrokinetic turbine inside a pipeline. We carried out CFD simulations and complemented them with experimental validation tests.

2 Problem Formulation

2.1 CAD Design

To carry out the present study, different turbine configurations were designed. Initially, a straight blade model was used as a starting point, and subsequently, two models were designed in which the blades tried to cover as much surface area as possible inside the tube. However, preliminary CFD simulations showed that the straight blade model was the most efficient. Figure 1 shows some of the different turbine models that have been developed, and Figure 2 shows the final design.

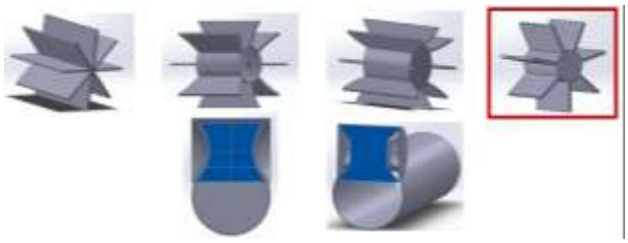

Fig. 1: Hydrokinetic turbine and Pipe CAD design

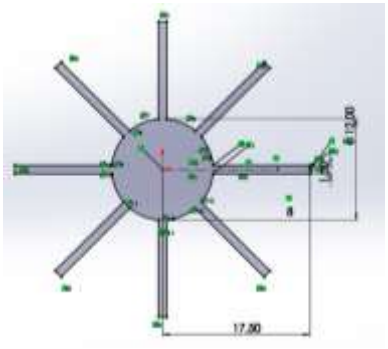

Fig. 2: Hydrokinetic turbine final design

After establishing the turbine model, modifications were made to the pipeline section designated for the installation of the turbine. Initially, an unmodified pipe design was used, resulting in a speed of 480 rpm. For the subsequent design, the area of the pipe where the turbine would be installed was narrowed to increase flow acceleration, to achieve a higher speed. The turbine was positioned in the narrowed section during the initial attempt and achieved approximately 950 rpm. However, the downstream flow exhibited excessive turbulence. As such, the turbine was repositioned in the central area of the constriction, resulting in a speed exceeding 4000 rpm and reduced turbulence compared to the previous scenario. This process is shown in Figure 3.

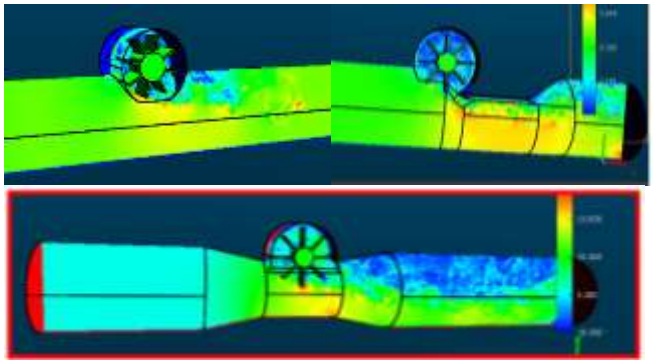

Fig. 3: Pipe designs and turbine positioning

To avoid calculation errors due to high pressures in small cavities resulting from CAD assembly, all gaps were eliminated in the final

assembly. Moreover, friction between parts was not considered.

This final configuration took advantage of the Venturi effect, which allowed for an acceleration of the turbine. It was designed as a 3-piece assembly that allowed the use of only one pipe with interchangeable pieces. The system was also designed so it could be manufactured and coupled into a sensorized test rig (Figure 4).

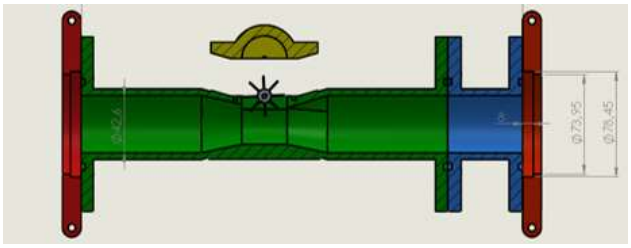

Fig. 4: Hydrokinetic turbine and pipe final design

2.2 Simulation Setup

The CFD study was carried out using the SIMULIA XFlow software, which uses a Lagrangian approach with the Lattice-Boltzmann methodology.

To simulate the hydrokinetic turbine inside the designed pipeline, the internal flow option was chosen. The turbine had a 35 mm diameter in all cases, and the pipe had a length of 295 mm. This length is adequate for examining the flow downstream of the turbine to determine if there is excessive turbulence and if the need arises to adjust the boundary conditions. Initially, these conditions establish a fixed rotational speed for the turbine of 1500 rpm and a flow rate of 28.83 m^3/h. A uniform lattice size of 0.5 mm is used for the meshing and no remeshing will be necessary during the simulation. The software uses the Courant number as a time step, which is the ratio of the time interval to the residence time in a finite volume. This parameter is essential as it affects the numerical stability of the simulation methods employed. In this particular simulation, a value of 0.5 was selected. Figure 5 provides a visualization of the simulation's discretization.

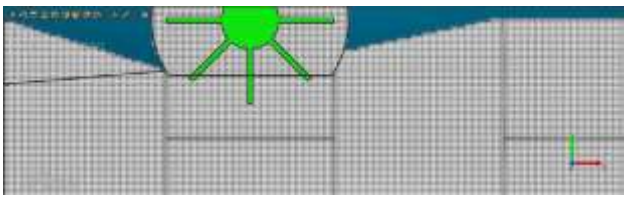

Fig. 5: Lattice size

The configuration of the simulations was established through prior work. Parameters were adjusted until a stable and reliable simulation model was reached. Figure 6 displays the velocity distribution and generated vorticity obtained via simulation.

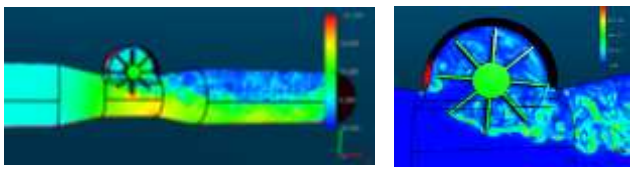

Fig. 6: Velocity distribution and vorticity generated

Once the reference parameters were obtained to carry out the simulations, it was decided to test three different turbine heights to see which distance was more favorable to obtain greater power in the design. Specifically, distances of 15, 18, and 21 mm measured from the center of the turbine concerning the longitudinal axis of the pipe were studied. The results revealed that at a height of 21 mm higher angular velocities are obtained for the same torque.

2.3 Experimental Study

This device consists of two differentiated parts: a coupling with a geometry that tries to take advantage of the Venturi effect to accelerate the water in the place of contact with the turbine and a turbine-generator set as shown in Figure 7.

Fig. 7: Installation configuration

Due to the physical limitation of the test panel, the experiments were conducted by varying the flow rate and without brake torque to avoid breakage of the turbine prototype. Thus, turbine models of 10, 8, and 6 blades were used.

The manufacturing process was done mainly by 3D printing, using a FabPro1000 3D resin printer and a Markforged Onyx 3D fiber carbon 3D printer. In the first case the updated design shown in Figure 6 was required to meet the printer's limitations. Furthermore, most of the extra structural elements (axle, DC motor) were also supplied by the university's workshops and only bearings and bolts had to be bought.

The carbon fiber device shown in Figure 8 was first fabricated, however when tested, the porosity due to how the material was printed caused

permanent and significant leakage in working conditions across the entire surface of the material. Therefore, the results obtained were discarded and the experimentation focused on the resin device.

Fig. 8: Manufactured fiber carbon device

The experimentation was carried out in the pipe test benches of the Fluid Mechanics lab at the Public University of Navarra (UPNA) as it is shown in Figure 9.

Fig. 9: Final installation of the resin device

The rotational speed was measured as a function of the flow rate passing through the device during the tests. The flow rate was measured using an electromagnetic flowmeter. The turbine's rotational speed was measured by attaching a plastic cylinder with adhesive to the turbine shaft. This setup, along with a digital tachometer, allowed for the measurement of the number of revolutions. Additional checks were performed using a stroboscope. The results obtained are shown in Figure 10.

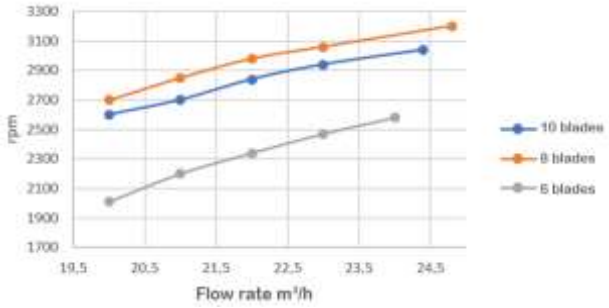

Fig. 10: Experimental RPM vs Flow rate results

To qualitatively measure the electrical power generated, a DC motor was attached to the cylindrical part and used to power LED devices installed on an electronic board.

3 Problem Solution

A validation of the CFD model was carried out with 8 and 10-bladed turbines where the runaway speed was measured under different water flows, and then compared with CFD results. Validation for the 8-blade and 10-blade turbine is shown in Figure 11.

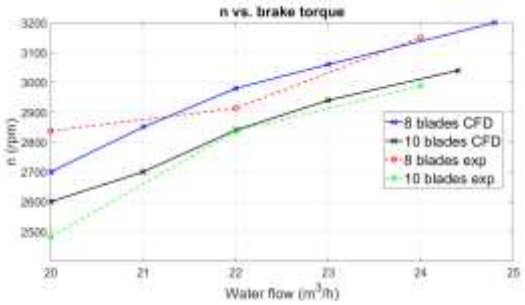

Fig. 11: RPM vs. Flow rate in experimentation and CFD

In Figure 11 it can be observed that the error between the experimental data and CFD is less than 10% at higher flow rates. It is considered that with errors <10% for higher flows and considering all the uncertainty that comes with these types of experimentations, the CFD model is validated.

Once the CFD models were validated, a study to observe their behavior under different braking moments was developed. For that, the defining parameters obtained in the validation process were kept the same, so the models were still valid.

For the CFD simulations design, statistical techniques based on the Design of Experiments (DOE) were employed. The selected design was a 22-second-order model with one central point and four additional star points. Moreover, the design factors were the number of blades and the braking torque, while the two response variables were the angular velocity and the power (shown in Equation (1)). The number of blades was set to 6 and 12 blades, while the torque levels were 0.01 and 0.027 N-m as presented in Table 1.

$$\text{Power (W)} = \text{Torque(Nm)} \cdot \omega \text{ (rad/s)} \qquad (1)$$

Table 1. DOE results

Nº blades	Torque (Nm)	Ang. velocity (rad/s)	Power (W)
10	0.027	244.42	6.60
10	0.0185	265.46	4.91
10	0.01	342.76	3.43
8	0.027	228.10	6.16
8	0.0185	249.69	4.62
8	0.0185	249.98	4.25
8	0.01	317.42	3.17
6	0.027	218.91	5.91
6	0.0185	231.10	4.28
6	0.01	336.68	3.37

Figure 12 shows the Pareto diagram for the speed analysis. It can be seen that the braking torque is the most significant factor with an inverse interaction, i.e. the higher the torque, the lower the revs. Likewise, it can also be seen that the number of blades of the turbine is a significant factor - although it is on the limit- and has a direct interaction, where the higher the number of blades, the higher the revolutions. The obtained results are highly reliable given the achieved adjusted R^2 of 95.9026% in this study. Also, the regression equation is shown in Equation (2).

$$RPM = 610.28 - 26.711 \cdot Nº\ Blades - 24251.9 \cdot Stroke + 1.68262 \cdot Nº\ Blades^2 + 285.677 \cdot Nº\ Blades \cdot Stroke + 431826 \cdot Stroke^2 \quad (2)$$

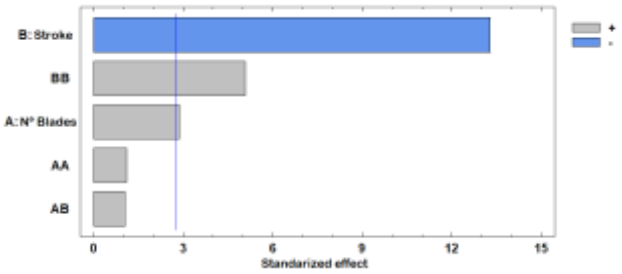

Fig. 12: Number of revolutions Pareto chart

Moreover, Figure 13 shows the Pareto diagram for the study of the power obtained in the turbine. According to this analysis, the torque and the number of blades are the two most significant factors with direct interaction. The obtained adjusted R^2 in this analysis was 99.1734%, indicating a very high level of reliability. Also, the regression equation is shown in Equation (3).

$$Power = 3.83968 - 0.371365 \cdot Nº\ Blades + 18.8339 \cdot Stroke + 0.0197486 \cdot Nº\ Blades^2 + 9.23378 \cdot Nº\ Blades \cdot Stroke + 2104.93 \cdot Stroke^2 \quad (3)$$

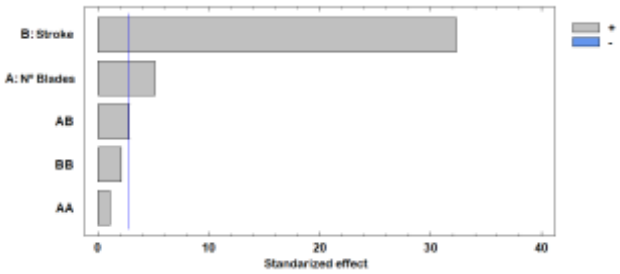

Fig. 13: Power Pareto chart

It should be pointed out that in both analyses the results obtained are coherent and coincide with the experimental and analytical studies of the vast majority of the articles analyzed in the introduction. Therefore, the simulations have been considered to be validated.

Figure 14 shows the graphical results attained from the DOE. It can be concluded that the 10-blade turbine delivers the most torque and operates at the highest speed. However, due to structural issues, the experimental test of the DOE was postponed.

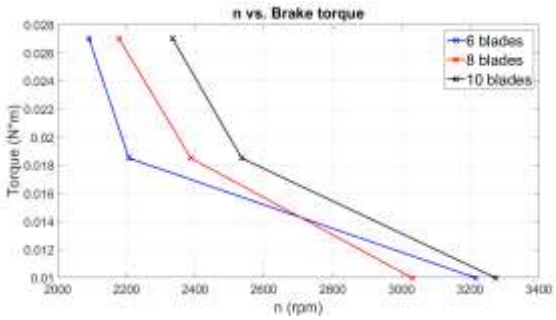

Fig. 14: RPM vs. torque in CFD

Finally, Figure 15 shows the circuit assembly for voltage measurement. The motor's two terminals are connected to the Ariston board and then to a multimeter (Figure 16). A 10 kΩ resistor is placed between the terminals to calculate the current flowing through the circuit using Ohm's law.

Fig. 15: Motor connection to the board

Fig. 16: Multimeter for voltage, current, and resistance measurement

The current measured by the multimeter is the same as the calculated current. The generation of electrical energy was verified by placing LED bulbs, as shown in Figure 17.

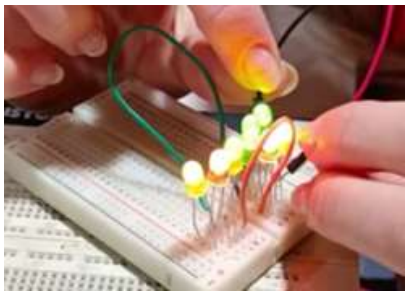

Fig. 17: Led bulbs

4 Conclusion

In the present study, different CAD designs of the device and CFD simulations with the SIMULIA XFlow software have been carried out. With that base and after a design and optimization process, a geometry with a narrowing in the central area was chosen to take advantage of the Venturi effect and generate electrical energy. Likewise, various turbine models were generated to get the maximum efficiency and finally, a straight 8-bladed geometry was chosen.

A whole design process, manufacture, and testing was carried out, all using the university's resources, such as 3D printers and test rigs. After testing a prototype made of carbon fiber, it was decided to discard it due to the excessive porosity of the material and all the components were manufactured by 3D printing in PET and the pipe in resin to avoid leakages.

A final validation of the CFD model was achieved with errors dropping below 10% for high flows.

Finally, to find the optimal configuration that allows for a greater generation of electricity, a design of experiments with CFD simulations was carried out under certain conditions of torque and number of blades. However, due to structural problems in the model, it could not be implemented in the experimental tests.

As a potential development for future work, it is considered interesting to be able to couple a programmable 4-quadrant motor to introduce the breakaway torque. In addition, conducting pressure differential measurements upstream and downstream of the turbine would allow for a more accurate analysis of the device's efficiency, based on an extensive literature review. Finally, ordering an external manufacture of the turbine and the pipe could result in better structural integrity and the elimination of whatever leakage there could be. Given the successful correlation between CFD simulations and experimentation, new designs will be implemented in domestic piping systems and eventually at the urban level.

References:

[1] Paish, O., Small hydro power: technology and current status, *Renewable and Sustainable Energy Reviews*, Vol.6, 2002, pp. 537-556.

[2] Osorio, J.F.S., Energías renovables, Ed. Prensas Universit. Zaragoza, 2008, ISBN: 978-84-16933-31-0.

[3] Khan, M.J., Bhuyan, G., Iqbal, M.T., Quaicoe, J.E., Hydrokinetic energy conversion systems and assessment of horizontal and vertical axis turbines for river and tidal applications: A technology status review, *Applied Energy*, Vol.86 (10), 2009, pp. 1823-1835.

[4] Nicholas, B.P., Laws, D., Hydrokinetic energy conversion: Technology, research, and outlook, *Renewable and Sustainable Energy Reviews*, Vol. 57, 2016, pp. 1245-1259.

[5] Niebuhr, C.M., van Dijk, M., Neary, V.S., Bhagwan, J.N., A review of hydrokinetic turbines and enhancement techniques for canal installations: Technology, applicability and potential, *Renewable and Sustainable Energy Reviews*, Vol.113, 2019, 109240.

[6] Riglin, J., Carter, F., Oblas, N., Schleicher, W.C., Daskiran, C., Oztekin, A., Experimental and numerical characterization of a full-scale portable hydrokinetic turbine prototype for river applications, *Renewable Energy*, Vol.99, 2016, pp. 772-783,

[7] Ibrahim, W.I., Mohamed, M.R., Ismail, R.M.T.R., Leung, P.K., Xing, W.W., Shah, A.A., Hydrokinetic energy harnessing

technologies: A review, *Energy Reports*, Vol.7, 2021, pp. 2021-2042.

[8] Álvarez-Álvarez, E., Rico-Secades, M., Fernández-Jiménez, A., Hydrodynamic water tunnel for characterization of hydrokinetic microturbines designs, *Clean Techn Environ Policy*, Vol.22, 2020, pp. 1843–1854.

[9] Silva dos Santos, I.F., Ramirez Camacho, R.G., Tiago Filho, G.L., Barkett Botan, A.C., Amoeiro Vinent, B., Energy potential and economic analysis of hydrokinetic turbines implementation in rivers: An approach using numerical predictions (CFD) and experimental data, *Renewable Energy*, Vol.143, 2019, pp. 648-662,

[10] Gautam, S., Sedai, A., Dhakal, R., Kumar Sedhai, B., Pol, S., CFD analysis of gravity-fed drag-type in-pipe water turbine to determine the optimal deflector-to-turbine position, *International Journal of Low-Carbon Technologies*, Vol.18, 2023, pp. 55–68,

[11] Park, J., Knight, B.G., Liao, Y., Mangano, M., Pacini, B., Maki, K.J., Martins, J.R., Sun, J., Pan, Y., CFD-based design optimization of ducted hydrokinetic turbines, *Sci Rep*, Vol.13, 2023, pp. 17968.

[12] Riyaz, N., Yee, C., Shihab, M., Oguz, E., Potential and prospects of hydrokinetic energy in Malaysia: A review, *Sustainable Energy Technologies and Assessments*, Vol.52 (C), 2022, 102265.

[13] Da Costa Oliveira, C.H., Cavalcanti Barros, M.L., Castelo Branco, D.A., Soria, R., Colonna Rosman, P.C., Evaluation of the hydraulic potential with hydrokinetic turbines for isolated systems in locations of the Amazon region, *Sustainable Energy Technologies and Assessments*, Vol.45, 2021, pp. 101079.

[14] Posa, A., Broglia, R., Analysis of the momentum recovery in the wake of aligned axial-flow hydrokinetic turbines, *Physics of Fluids*, 2022, Vol.34 (10), pp. 105130.

[15] Hasanzadeh N., Payambarpour S.A., Najafi A.F., Magagnato F., Investigation of in-pipe drag-based turbine for distributed hydropower harvesting: Modeling and optimization, *Journal of Cleaner Production*, Vol. 298, 2021.

[16] Monsalve O.D., Graciano J., Zuluaga D.A.H., Numerical Simulation of a Propeller-Type Turbine for In-Pipe Installation, *Journal of Advanced Research in Fluid Mechanics and Thermal Sciences*, Vol. 83, No.1, 2021, pp. 1–16.

[17] Muratoglu, A., Demir, M.S., Modeling spherical turbines for in-pipe energy conversion, *Ocean Engineering*, Vol.246, 2022, pp. 110497.

[18] Climent, M., Microturbine that uses water from pipes to generate power. *El Mundo*, (30/07/2014), [Online]. https://www.elmundo.es/economia/2014/07/30/53d7e040ca4741c46d8b45a3.html#:~:text=Las%20microturbinas%20explotan%20el%20agua,red%20o%20utilizada%20para%20autoconsumo (La microturbina que usa el agua de las tuberías para generar energía), (Accessed Date: February 12, 2024).

[19] Pipe waterwheel generates electricity from the house tap, Ingenieros Técnicos, (04 10 2014). http://www.ingeniostecnicos.com/2014/10/ES-Pipe-waterwheel-genera-electricidad-con-el-grifo-de-casa.html (Pipe waterwheel genera electricidad con el grifo de casa), (Accessed Date: February 12, 2024).

[20] Team, Purdue ECT, LUCIDPIPE™ POWER SYSTEM, *ECT Fact Sheets*, 2016, 224, http://dx.doi.org/10.5703/1288284316353.

[21] Gava, K. F., An analysis of the LucidPipe™ Power System in cities in Paraná, Bachelor's thesis, Universidade Tecnológica Federal do Paraná, 2018. (Uma análise do LucidPipe™ Power System em cidades paranaenses)

[22] Farb, D., Turbine relationships in pipes (patent), 2009, [Online]. https://patents.google.com/patent/US20110140434A1/en (Accessed Date: February 15, 2024).

[23] Farb, D., Van Zwaren, J., Farkash, A., Kolman, K., Hydroelectric in-pipe turbine blades (patent), 2010, [Online]. https://patents.google.com/patent/WO2010136978A3/no (Accessed Date: February 15, 2024).

[24] Farb, D., Benkatina hydroelectric turbine: alterations of in-pipe turbines (patent), 2011, [Online]. https://patents.google.com/patent/US20110188990A1/en (Accessed Date: February 15, 2024).

[25] Montgomery, J.S., In-pipe turbine (patent), 2012, [Online]. https://patents.google.com/patent/US20120274066A1/en?oq=13458866 (Accessed Date: February 15, 2024).

[26] Nakamura, K., Toshimasa, M., Satoru, K., So, K., Takuya, T., Takanori, T., Naritoshi, N.,

Water turbine and pipe (patent), 2015, [Online]. https://patents.google.com/patent/JP2015178829A/en?oq=JP2015178829 (Accessed Date: February 15, 2024).

[27] Min, L.S., Pipe type small hydropower generation apparatus (patent), 2020, [Online]. https://patentscope.wipo.int/search/es/detail.jsf?docId=KR309456947&_cid=P12-LSMDUM-04572-1 (Accessed Date: February 15, 2024).

Contribution of Individual Authors to the Creation of a Scientific Article (Ghostwriting Policy)

The authors equally contributed to the present research, at all stages from the formulation of the problem to the final findings and solution.

Sources of Funding for Research Presented in a Scientific Article or Scientific Article Itself

No funding was received for conducting this study.

Conflict of Interest

The authors have no conflicts of interest to declare.